



# Harmonic strain-optical response revealed in the isotropic (liquid) phase of liquid crystals

P Kahl, P Baroni, Laurence Noirez

► **To cite this version:**

P Kahl, P Baroni, Laurence Noirez. Harmonic strain-optical response revealed in the isotropic (liquid) phase of liquid crystals. Applied Physics Letters, American Institute of Physics, 2015, <10.1063/1.4929321>. <hal-01353743>

**HAL Id: hal-01353743**

**<https://hal.archives-ouvertes.fr/hal-01353743>**

Submitted on 12 Aug 2016

**HAL** is a multi-disciplinary open access archive for the deposit and dissemination of scientific research documents, whether they are published or not. The documents may come from teaching and research institutions in France or abroad, or from public or private research centers.

L'archive ouverte pluridisciplinaire **HAL**, est destinée au dépôt et à la diffusion de documents scientifiques de niveau recherche, publiés ou non, émanant des établissements d'enseignement et de recherche français ou étrangers, des laboratoires publics ou privés.

## Harmonic strain-optical response revealed in the isotropic (liquid) phase of liquid crystals

P. Kahl, P. Baroni, and L. Noirez

Citation: [Applied Physics Letters](#) **107**, 084101 (2015); doi: 10.1063/1.4929321

View online: <http://dx.doi.org/10.1063/1.4929321>

View Table of Contents: <http://scitation.aip.org/content/aip/journal/apl/107/8?ver=pdfcov>

Published by the [AIP Publishing](#)

---

### Articles you may be interested in

[Electrically tunable refractive index in the dark conglomerate phase of a bent-core liquid crystal](#)

*Appl. Phys. Lett.* **104**, 021903 (2014); 10.1063/1.4861837

[Phase contrast imaging using photothermally induced phase transitions in liquid crystals](#)

*Appl. Phys. Lett.* **89**, 211116 (2006); 10.1063/1.2397030

[Orientational and interaction induced dynamics in the isotropic phase of a liquid crystal: Polarization resolved ultrafast optical Kerr effect spectroscopy](#)

*J. Chem. Phys.* **120**, 10828 (2004); 10.1063/1.1737293

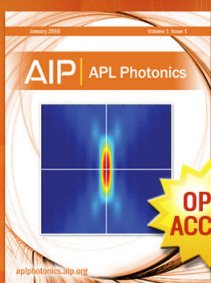
[Dynamics in supercooled liquids and in the isotropic phase of liquid crystals: A comparison](#)

*J. Chem. Phys.* **118**, 9303 (2003); 10.1063/1.1568338

[Liquid crystal dynamics in the isotropic phase](#)

*J. Chem. Phys.* **116**, 360 (2002); 10.1063/1.1423948

---



Launching in 2016!  
The future of applied photonics research is here

OPEN  
ACCESS

AIP | APL  
Photonics

## Harmonic strain-optical response revealed in the isotropic (liquid) phase of liquid crystals

P. Kahl, P. Baroni, and L. Noirez<sup>a)</sup>

Laboratoire Léon Brillouin (CEA-CNRS), CE-Saclay, Paris-Saclay University, 91191 Gif-sur-Yvette, France

(Received 10 June 2015; accepted 8 August 2015; published online 25 August 2015)

A strong optical birefringence is observed when applying a small amplitude oscillatory strain to the liquid phase of a liquid crystal. This unpredicted birefringence is found to oscillate at the same frequency as the driving frequency, with frequencies down to 0.01 Hz. This birefringence is visible up to 15 °C above the liquid crystal transition. This opto-dynamic property is interpreted as a result of a coupling of the orientational pretransitional fluctuations existing in the isotropic phase and long range elastic interactions recently identified in liquids. The conversion of the mechanical wave in an optical response is shapeable. Two examples of synchronized periodic signals are shown: the sine and the square waves. The optimization of the signal is analyzed using a Heaviside-step shear test. This optical property is immediately exploitable to design low energy on/off switching materials. © 2015 AIP Publishing LLC. [<http://dx.doi.org/10.1063/1.4929321>]

In liquid crystal (LC) displays, the tunable optical properties originate exclusively from the reorientation of the liquid crystalline domains. This is usually achieved by applying external fields as electric, magnetic, or mechanical fields.<sup>1</sup> No tunable properties were found at temperatures above the liquid crystal phases, i.e., in the isotropic phase. This phase is considered as an ordinary liquid.<sup>2,3</sup> Here, we reveal that the isotropic liquid is also convertible into an optically active material when it is stimulated at the sub-millimeter scale with a low frequency mechanical strain. These experiments suppose that a dynamic coupling exists between the pretransitional fluctuations (clusters of molecules with identical directions coexisting within the isotropic phase) and elastic properties uncovered at low frequency (typically below the Hz) in various liquids.<sup>4-9</sup> This strategy is efficient since a strong and reversible optical response is highlighted in the isotropic phase upon a low frequency low strain mechanical solicitation. This strain-induced optical birefringence is visible up to 15 °C above the isotropic transition and has the advantage of producing a true black phase between crossed polarizers in its inactivated state. This effect is synchronized with the excitation. Identified in the isotropic phase of several liquid crystalline fluids, this unknown effect is likely a generic property. We illustrate the emergence of optical birefringence in the isotropic phase on the non-exhaustive basis of a low molecular weight liquid crystal polymer (LCP95) in use for LC-displays in its liquid crystal phase.<sup>10</sup> This molecule exhibits a particularly strong optical signal in the isotropic phase. We first present optical signals displayed at different strain amplitudes and different temperatures in the isotropic phase. Three different birefringence regimes are identified by increasing the strain amplitude: in-phase with the strain, in-phase with the strain-rate, and anharmonic optical signals. A Heaviside-step shear test completes the analysis and enables to define the experimental conditions for which this elastic optical response is dynamically stable and robust. Two examples

of periodic signals (sine and square) illustrate the optical response to low frequency mechanical stimuli.

The sample (LCP95) is a 12 repetitive units acrylate backbone crafted with cyanobiphenyl ended side chains linked by a propyl spacer presenting an isotropic-smectic transition at  $T_{SAI} = 79.8 \pm 0.05$  °C. Its hydrodynamic radius determined by Light scattering is 1.4 nm. The isotropic phase exhibits the thermodynamic (Fig. 1(a)), conventional rheological (Fig. 1(b)), and symmetry characteristics of a simple liquid. This first order transition is resolved within  $\pm 0.05$  °C with an order parameter vanishing at the transition. The optical measurements are performed in transmission mode under crossed polarized microscopy (Olympus BX60). Oscillatory and step shear motion were applied using a home-improved CSS450 Linkam cell (temperature gradient  $< \pm 0.05$  °C) equipped with quartz plate-plate fixtures. The incident wavelength was  $\lambda = 614$  nm. The transmitted intensity  $I$  was normalized to the uncrossed polarizer intensity  $I_0$  and the averaged birefringence  $\Delta n$  is calculated using the transmittance:  $\frac{I}{I_0} = \sin^2(\langle \Delta n \rangle \frac{e}{\lambda})$ , where  $e$  is the gap thickness. A trigger device (by R&D Vision,  $10^{-9}$  s synchronization delay) measures simultaneously the strain amplitude and the transmitted intensity by using two individual CCD cameras (80 fps, Vision Technology) (Fig. 1(c)).

In a first series of experiments, the mechanical excitation is effected by applying a weak oscillatory strain stimulus at low frequency (typically from 0.01 Hz up to 2 Hz), i.e., close to equilibrium conditions. The input wave is a sinusoidal strain wave:  $\gamma(t) = \gamma_0 \sin(\omega t)$  of angular frequency  $\omega$  and strain amplitude  $\gamma_0$  defined as the ratio of the displacement length  $\Delta l$  to the sample thickness:  $\gamma_0 = \frac{\Delta l}{e}$ . Fig. 2 illustrates the optical response of the isotropic phase to a 0.5 Hz oscillatory excitation at +1 °C above the  $S_{AI}$  transition. The photo snapshots at the top of Fig. 2 correspond to the true colors emerging from the isotropic phase during the periodic solicitation. The optical birefringence indicates that a long range orientation of the molecules establishes. The isotropic phase is thus optically active as soon as the lowest frequencies, a property unknown in physics of liquid crystals above the phase

<sup>a)</sup>Email: laurence.noirez@cea.fr

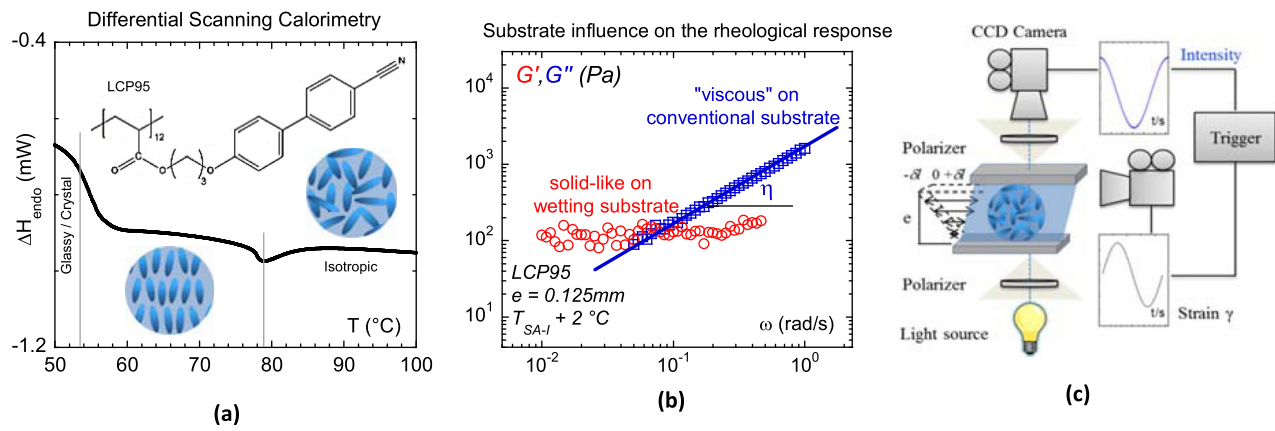


FIG. 1. (a) Differential scanning calorimetry on LCP95 indicates a first order smectic A to isotropic transition at  $79.8^{\circ}\text{C}$  (data recorded at  $+10^{\circ}\text{C}/\text{min}$ ). (b) Comparison of dynamic relaxation data of the LCP95 in the isotropic phase ( $T_{\text{SAI}} + 2^{\circ}\text{C}$ ,  $e = 120 \mu\text{m}$ , 1% strain amplitude, ARES2 rheometer): On conventional substrate (glass): The shear modulus is not measurable and loss modulus  $G''$  scales with  $\omega^2$  depicting a Newtonian behavior (blue squares ( $\square$ ); conventional glass substrate) and on wetting substrate (red circles ( $\circ$ ); alumina substrate): the shear modulus (elastic response)  $G'$  dominates at low frequency.<sup>7</sup> The storage modulus  $G'$  dominates indicating a low frequency elastic behavior. (c) Optical setup: The isotropic phase fills the gap between two fixtures and is observed between crossed polarizers with a microscope (magnification lens:  $\times 100$ ). The upper fixture moves backward-forward with a tens microns scale oscillatory amplitude. A trigger device enables the simultaneous measurement of the optical signal and the movement by 2 individual CCD cameras.

transitions. The analysis of the signal reveals that the optical birefringence wave is harmonic with the input signal and can therefore be modeled by a sine wave:  $\Delta n(\omega) = n_{\text{max}} \sin(\omega t + \varphi)$  with  $\varphi$  the phase-shift. For the applied shear frequency and a strain amplitude of  $\gamma_0 = 10\%$ , the signals almost superimpose with the strain rate  $\frac{\partial \gamma(t)}{\partial t} = \dot{\gamma}(t)\omega$ . Similar optical signals are obtained for various low strain amplitudes and different temperatures up to  $15^{\circ}\text{C}$  above the transition. The closer to the transition temperature, the more intense is the birefringence confirming the coupling to pretransitional fluctuations that melt by increasing the temperature. Fig. 3(a) displays the evolution of the birefringence (peak values) versus strain amplitude at  $+1^{\circ}\text{C}$  above the  $S_{\text{A1}}$ -I transition. The examination of the strain dependence of the optical signal indicates three regimes. At very low strain amplitudes ( $\gamma_0 \leq \gamma_{\text{crit}} \approx 4 \pm 1\%$ ), the optical signal is hardly detectable and is in-phase with the

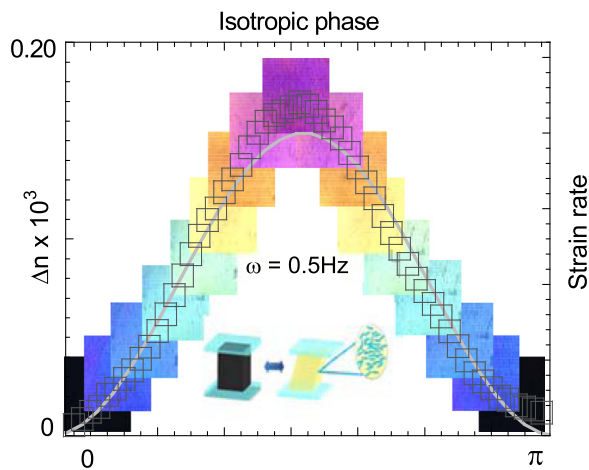


FIG. 2. Photo snapshots of the transmittance and corresponding birefringence (at  $\lambda = 614 \text{ nm}$ ) emerging upon a low frequency mechanical oscillation ( $\omega = 0.5 \text{ Hz}$ ) in the isotropic phase at  $T - T_{\text{SAI}} = +1^{\circ}\text{C}$  (sample thickness  $e = 250 \mu\text{m}$  and  $\gamma_0 = 10\%$ , the photographs are recorded between crossed polarizers). Corresponding input strain rate (grey continuous sine line  $\text{---}$ ) and induced birefringence (data points: black squares,  $\square$ , sine model fit). The birefringence is in-phase with the strain rate (phase shift about  $\varphi = 7^{\circ}$ ).

strain (inset (1) of Fig. 3(a)), i.e., in-phase elastic behavior. Above this weak critical strain amplitude ( $4\% < \gamma_0 < 30\%$ ), the birefringence increases linearly with strain amplitude. This linearity with the strain parameter is observed on all probed temperatures (Fig. 3(b)) confirming the direct dependence on the strain parameter. In this regime, the optical signal is nearly in-phase with the strain rate (inset (2) of Fig. 3(a)) with a phase shift close to  $10^{\circ}$ . At higher strains ( $\gamma_0 > 30\%$  at  $+1^{\circ}\text{C}$ ), the peak value of the birefringence does not evolve anymore (plateau values). The optical signal does not relax to the baseline between two successive periods (inset (3)), and the shape of the wave is splitted indicating the generation of a second harmonic and possibly a third harmonic of half period. The further increase of the strain amplitude generates the superposition of multiple harmonics giving rise to an apparent continuous-like birefringent signal whose asymptotic value is the flow birefringence (inset (4)). The conditions are equivalent to a steady state flow whose effects are already known.<sup>11–14</sup> In contrast to these far out-of-equilibrium conditions, at low frequency and low strain amplitude, the isotropic phase is close to an equilibrium state where no mechanical coupling is expected (the lifetimes  $\tau$  of the pretransitional fluctuations determined by Kerr effects are of the order of  $\tau \approx 10^{-9} \text{ s}$  for rod-like liquid crystals<sup>15</sup> down to  $\tau \approx 10^{-4} \text{ s}$  for liquid crystal polymers<sup>16</sup>). In the low frequency harmonic regime (where the sine wave is conserved), a reduced dynamic birefringence  $\Delta n^* = \frac{\Delta n}{\gamma_0 - \gamma_{\text{crit}}}$ , can be defined by renormalizing the birefringence by the reduced strain value  $\gamma_0 - \gamma_{\text{crit}}$ .  $\gamma_{\text{crit}}$  defines the frontier separating the very low strain regime where the birefringent signal is weak and in phase with the applied strain wave from the strain regime where the optical signal is in phase with the strain rate and increases rapidly with the strain. In the second regime (above  $\gamma_{\text{crit}}$ ), the evolution of the reduced birefringence  $\Delta n^*$  highlights a strain regime where the dynamic birefringence is independent of the applied strain amplitude (Figs. 3(b) and 3(c)). Being independent of the external stimuli (the strain), this quantity is linked to an elastic character of the material.



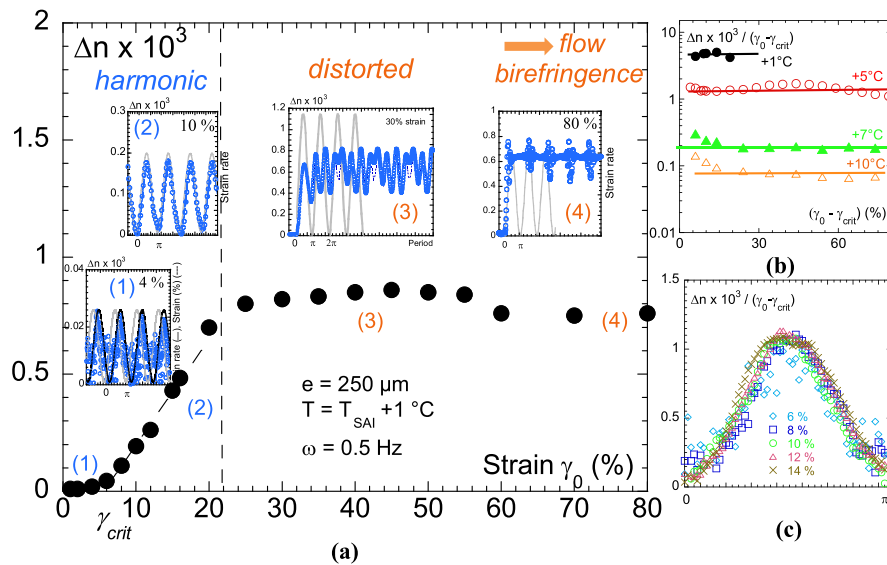


FIG. 3. (a) Strain dependence of the birefringent signal (peak value) in the isotropic phase ( $T - T_{SAI} = +1^\circ\text{C}$ ) at low frequency oscillatory excitation ( $\omega = 0.5\text{ Hz}$ , sample thickness  $e = 250\ \mu\text{m}$ ). The corresponding oscillatory signals are shown as insets for 4% (1), 10% (2), 30% (3), and 80% (4) strain amplitude. The applied frequency is the same for all insets ( $\omega = 0.5\text{ Hz}$ ) and is represented by the continuous grey curve.  $\gamma_{crit}$  defines the frontier separating the very low strain regime where the birefringent signal is in phase with the applied strain wave from the strain regime where the optical signal is in phase with the strain rate and increases linearly up to 30% strain amplitude. Above 30% strain amplitude (inset (3)), the optical signal does not relax and is splitted indicating the generation of a second harmonic and possibly a third harmonic of half period (fitted by a dashed line), and at higher strains, the generation of multiple harmonics (4) flatten the signal to an asymptotic value corresponding to the flow birefringence. (b) Invariance of the reduced birefringence  $\Delta n / (\gamma_0 - \gamma_{crit})$  with the strain amplitude observed at different temperatures:  $+1^\circ\text{C}$  (●),  $+5^\circ\text{C}$  (○),  $+7^\circ\text{C}$  (▲), and  $+10^\circ\text{C}$  (△). (c) The superposing oscillatory signals of the reduced birefringence at  $+3^\circ\text{C}$  above  $T_{SAI}$  for various strain amplitudes.

A second series of mechanical measurements consists in probing the optical response of the isotropic phase to a Heaviside step excitation.<sup>17</sup> This step excitation allows the determination of the conditions of optimization of the transfer function from the mechanical motion to the optical response.<sup>18</sup> It gives a condensed overview of the expected dynamic behavior (even if the cutoff frequency is not experimentally accessible). This test is carried out experimentally by applying a sudden constant shear rate at  $t_0$ . A detailed illustration of the time-dependent evolution at a low shear rate of  $3\text{ s}^{-1}$  is found together with the step function in Fig. 4(a). Different shear rates have been tested indicating a similar behavior (inset of Fig. 4). The highest birefringence (optimized gain) found before the development of instabilities is

obtained at around:  $\dot{\gamma} = 30\text{ s}^{-1}$ . In terms of signal processing theory, the response to the Heaviside step function can be considered to be of first order and therefore modeled by  $\Delta n(t) = K(1 - e^{-t/\tau})$ , with  $\tau_{off}$  the cutoff time and  $K$  the gain. As a response to the step function, the birefringence rises exponentially with corresponding cutoff times  $\tau_{off}$  lower than 200 ms before saturating. The latter is the maximal intensity that can be obtained for a specific excitation.  $\tau$  and  $K$  indicate how fast and how much the liquid is able to respond instantly to the sudden signal. The cutoff frequency is  $\omega_{c.o.} = \frac{1}{\tau_{off}} \cong 20\text{ Hz}$ . It is the maximum frequency value above which the signal starts to attenuate. In analogy with electronic filters, the birefringence behavior is similar to a capacitor and a resistor in series,<sup>18</sup> i.e., a low-pass filter. Below

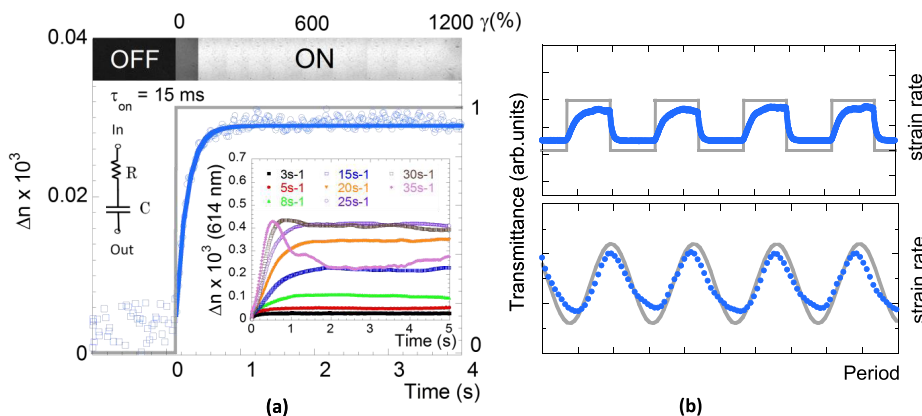


FIG. 4. (a) Input step function (grey continuous line, —) and birefringent signal (data points: blue circles, ○, exponential model fit, blue continuous line, —) in the isotropic phase at  $+1^\circ\text{C}$  above  $T_{SAI}$  for a sample thickness  $e = 250\ \mu\text{m}$  and shear rate  $\frac{d\dot{\gamma}}{dt} = 3\text{ s}^{-1}$ . Top of the figure: transmittance during the step function (photographs recorded between crossed polarizers with a monochromatic incident light). The isotropic phase behaves as a low pass filter with a resistor R and a capacity C. (b) Optical response (data points: blue filled circles, ●) synchronized to a sine and a square input strain rate waves (grey continuous line, —).

this cut-off frequency, the output signal stays in-phase in respect to the solicitation. At low frequencies  $\omega < \omega_{c,o}$ , the isotropic phase is therefore supposed to react elastically. This is confirmed by the harmonic behavior observed in the oscillatory experiments discussed above.

In conclusion, we have highlighted that, at the sub-millimeter scale, the isotropic phase of an ordinary liquid crystal behaves as a low frequency optical oscillator in response to a mechanical stimulation of frequencies as low as 0.01 Hz. The reversible synchronized birefringent response, whose intensity is directly linked to the strain amplitude, indicates an elastically driven behavior. The synchronized orientation of molecules, i.e., the strain field produces a long range organized material and its relaxation back to the isotropic liquid once the stress is removed indicate that the oscillatory strain produces a variation of entropy of the system (loss of entropy (during the orientation) and entropy gain (during relaxation)). This effect is possible if the pretransitional fluctuations are correlated at the scale of the sample in the isotropic liquid. In other words, the isotropic phase behaves dynamically as an elastic medium.<sup>19</sup> This synchronized birefringence is coherent with the stress results observed at low strain amplitudes on various liquids indicating an elastic pre-regime existing at the sub-millimeter scale prior to the conventional flow or viscous behavior.<sup>4-9</sup> This low frequency elastic plateau is also identified in the isotropic phase of LCP95 as illustrated in the stress measurements carried out at 0.200 mm on wetting substrate (Fig. 1(b)) and in agreement with previous results.<sup>4-9</sup> Finally, the birefringence induced in the isotropic phase cannot be interpreted as a surface induced property. Wall or capillary effects rule out since the probed gap distances far exceed coherence lengths of the order of several nanometers.<sup>3,20-22</sup> The birefringence instantly relaxes to its initial state (which appears black between crossed polarizers) demonstrating that no preorientation exists but that it has its origin in the reorientation of pretransitional fluctuations that are correlated in an elastic bulk. In the literature, orientational pretransitional fluctuations of rod-like liquid crystals exhibit lifetimes in the isotropic phase are of the order of  $\tau \approx 10^{-9}$  s for the rod-like liquid crystals,<sup>15</sup> necessitating frequencies of the order of  $10^9$  Hz to induce a coupling with these timescales. In LCPs, the orientational pretransitional fluctuations announce lifetimes lying around  $\tau \approx 10^{-4}$  s (Ref. 16) which still demand MHz solicitation frequencies. The present study reveals that the isotropic phase responds to a mechanical stimulation down to the tenth of the Hertz. Therefore, the pretransitional fluctuations are not free but elastically correlated in the isotropic liquid. Correlatively, the pretransitional fluctuations serve as a dynamic optical probe to “visualize” long range elastic interactions in the liquid. Weak intermolecular interactions (of about several Pa) can thus form a delicate elastic network up to a macroscopic scale. The interplaying forces are weak, fundamentally different from those governing LC-elastomer networks<sup>23-25</sup> but not negligible at the sub-millimeter scale. The free energy of the isotropic phase might be approximated by integrating a term coupling the orientational pretransitional fluctuations to the strain (at weak strain amplitudes):  $F = F_0 + 1/2.G_0.\gamma^2 - \sigma.\gamma - k.S(\gamma).\gamma$ , where  $S$  is the order parameter assumed proportional to the birefringence ( $S \cong 0$

without strain),  $G_0$  is the weak shear modulus identified in the isotropic phase<sup>4-8</sup> (linked to the Young modulus),  $\sigma$  is the applied stress, and  $k$  is a constant coupling the order parameter to the strain  $\gamma$ . This expression indicates that the energy is lowered under strain via an increase of the order parameter (birefringence) and thus an entropy decrease. The stress release produces an entropy gain and a return to the isotropic state. This mechanism sets the role of long range reversible (elastic) interactions as crucial in the liquid state. In molecular liquids, noteworthy theoretical approaches consider a solidlike continuum<sup>26</sup> and even predict the elasticity, at several molecular length scale<sup>27</sup> or even macroscopically, the strength of which depends on the network size,<sup>28</sup> in particular, on the interactions between molecules.<sup>28-30</sup> Finally, this low frequency property consumes little energy (the liquid is stimulated close to its equilibrium state) and can serve as an excellent basis for LC-displays exhibiting a mechano-induction from a true black state to a birefringent state between crossed polarizers.

The authors are grateful to R&D Vision for the trigger software.

- <sup>1</sup>Handbook of Liquid Crystals, 2nd ed., edited by J. W. Goodby, P. J. Collings, T. Kato, C. Tschierske, H. Gleeson, and P. Raynes (John Wiley & Sons, 2014), Vol. 8.
- <sup>2</sup>G. Marrucci and F. Greco, Adv. Chem. Phys. **86**, 331 (1993).
- <sup>3</sup>The Physics of Liquid Crystals, 2nd ed., edited by P. G. de Gennes and J. Prost (Oxford University Press, Oxford, 1993).
- <sup>4</sup>B. V. Derjaguin, U. B. Bazarov, K. T. Zandanova, and O. R. Budaev, Polymer **30**, 97–103 (1989).
- <sup>5</sup>L. Noirez and P. Baroni, J. Phys.: Condens. Matter **24**, 372101 (2012).
- <sup>6</sup>L. Noirez, Phys. Rev. E **72**, 51701 (2005).
- <sup>7</sup>L. Noirez, H. Mendil-Jakani, P. Baroni, and J. H. Wendorff, Polymers **4**, 1109 (2012).
- <sup>8</sup>H. Mendil, P. Baroni, and L. Noirez, Eur. Phys. J. E **19**, 77 (2006).
- <sup>9</sup>P. Kahl, P. Baroni, and L. Noirez, Phys. Rev. E **88**, 50501 (2013).
- <sup>10</sup>L. D. Farrand, J. Patrick, and S. A. Marden, “Mesogenic compounds, liquid crystal medium and liquid crystal display,” Merck Patent GmbH EP1690917 B1, 8 Oct. 2008.
- <sup>11</sup>V. Zvetkov, Acta Phys. Chim. **19**, 86 (1944).
- <sup>12</sup>C. Pujolle-Robic and L. Noirez, Nature **409**, 167 (2001).
- <sup>13</sup>C. Bailey, K. Fodor-Csorba, R. Verduzco, J. T. Gleeson, S. Sprunt, and A. Jákli, Phys. Rev. Lett. **103**, 237803 (2009).
- <sup>14</sup>C. Sadron, J. Phys. Radium **8**, 481 (1937).
- <sup>15</sup>S. J. Rzoska, A. Drozd-Rzoska, P. K. Mukherjee, D. O. Lopez, and J. C. Martinez-Garcia, J. Phys.: Condens. Matter **25**, 245105 (2013).
- <sup>16</sup>V. Reys, Y. Dormoy, J. L. Gallani, P. Martinoty, P. Le Barny, and J. C. Dubois, Phys. Rev. Lett. **61**, 2340 (1988).
- <sup>17</sup>G. L. Anderson, J. Sound Vib. **34**, 425 (1974).
- <sup>18</sup>B. Brogliato, R. Lozano, B. Maschke, and O. Egeland, Dissipative Systems Analysis and Control, 2nd ed. (Springer Verlag, London, 2007).
- <sup>19</sup>G. Astarita, Polym. Eng. Sci. **14**, 730 (1974).
- <sup>20</sup>B. Chu, C. S. Bak, and F. L. Lin, Phys. Rev. Lett. **28**, 1111 (1972).
- <sup>21</sup>G. S. Iannacchione and D. Finotello, Phys. Rev. Lett. **69**, 2094 (1992).
- <sup>22</sup>B. Jérôme, A. Bosseboeuf, and P. Pieranski, Phys. Rev. A **42**, 6032 (1990).
- <sup>23</sup>P. G. de Gennes, C. R. Acad. Sci. Paris **281**, 101 (1975).
- <sup>24</sup>E. M. Terentjev and M. Warner, Eur. Phys. J. E **4**, 343 (2001).
- <sup>25</sup>S. Nikolov, C.-S. Han, and D. Raabe, Int. J. Solids Struct. **44**, 1582 (2007).
- <sup>26</sup>A. V. Granato, Mater. Sci. Eng., A **521–522**, 6 (2009).
- <sup>27</sup>M. Schoen, S. Hess, and D. J. Diestler, Phys. Rev. E **52**, 2587 (1995).
- <sup>28</sup>F. Volino, Ann. Phys. **22**, 18 (1997).
- <sup>29</sup>J. P. Ibar, Z. Zhang, Z. M. Li, and A. Santamaria, J. Macromol. Sci., Part B: Phys. **54**, 649 (2015).
- <sup>30</sup>S. Droulias, A. G. Vanakaras, and D. J. Photinos, Liq. Cryst. **37**, 969 (2010).